J|A|C|S
ARTICLES
Published on Web 08/26/2003

Inelastic Neutron Scattering and Raman Spectroscopies and Periodic DFT Studies of Rb_2PtH_6 and Rb_2PtD_6

Stewart F. Parker,*[,†] Stephen M. Bennington,[†,○] Anibal. J. Ramirez-Cuesta,[†,#] Gudrun Auffermann,[‡,▽] Welf Bronger,[§,◆] Henryk Herman,[||,+] Kenneth P. J. Williams,[⊥,∞] and Tim Smith[⊥,¶]

Contribution from the ISIS Facility, Rutherford Appleton Laboratory, Chilton, Didcot, Oxon OX11 0QX, United Kingdom; Max Planck Institut für Chemische Physik fester Stoffe, Nöthnitzer Straβe 40, 01187 Dresden, Germany; Institut für Anorganische Chemie der TH Aachen, Prof.-Pirlet-Str. 1, 52056 Aachen, Germany; Department of Chemistry, University of Surrey, Guildford, Surrey GU2 5XH, United Kingdom; and Spectroscopy Products Division, Renishaw plc, Old Town, Wotton-under-Edge, Gloucestershire GL12 7DL, United Kingdom

Received January 24, 2003; E-mail: S.F.Parker@rl.ac.uk

Abstract: The present work has provided a complete set of assignments for the vibrational spectrum of Rb_2PtH_6 and Rb_2PtD_6. To confirm the assignments, a periodic density functional theory (DFT) code has been applied to the analysis of the inelastic neutron scattering (INS) spectrum of an ionic material for the first time. The work has also provided an explanation for the unusual infrared spectrum of the potassium salt. The most significant aspect of the work is the use of the momentum transfer information provided by an INS chopper spectrometer. The straightforward method employed for the analysis of the data is applicable to *any* molecular system (organic or inorganic) and demonstrates the potential of these instruments for chemistry. Periodic DFT was also used to study the other A_2PtH_6 (A = alkali metal) including, the at present, unknown Li salt, which is found to be stable. The DFT studies have also highlighted the crucial role of the cation in removing charge from the transition metal and "hydride" ligand. It is suggested that this is a general occurrence.

I. Introduction

Metal hydride complexes are of considerable interest for hydrogen storage applications,[1] and in recent years, a large number of compounds of the general formula A_xMH_y (A = alkali metal or earth, M = transition metal, $x = 1-4$, $y = 2-10$) have been synthesized.[2,3] Recent work has shown that it is possible to make hydride complexes in high oxidation states of second and third row transition metals by using high hydrogen pressures (>1500 bar) in the temperature range from 770 to 920 K.[3] Rb_2PtH_6 (= $\{Rb^+\}_2$ $[PtH_6]^{2-}$) and its deuteride are formally Pt(IV) and thus offer the opportunity of examining the bonding for the simplest possible ligand, H^-. Vibrational spectroscopy provides a straightforward way to investigate the bonding experimentally. In the present work, we have used a combination of Raman and inelastic neutron scattering (INS) spectroscopies to determine all of the internal modes and most of the external modes of the compounds. In the course of this work, we have developed a novel approach to the analysis of the INS spectrum that enables impurities to be detected and unambiguous distinction of fundamentals from higher-order transitions. To confirm the assignments and provide some insight into the bonding, we have used a periodic density funtional theory (DFT) code to model the A_2PtH_6 (A = alkali metal) compounds including the, at present, unknown Li salt.

II. Experimental Section

A. Synthesis of the Compounds. Polycrystalline samples of Rb_2PtH_6 and Rb_2PtD_6 were synthesized by the reaction of RbH/D (itself prepared by direct reaction of the elements in an autoclave) with platinum sponge in hydrogen or deuterium gas at 1500−1800 bar and 770 K as described in detail elsewhere.[4] The compounds are extremely air and moisture sensitive so were sealed in custom-made $50 \times 30 \times 5$ mm^3 quartz cuvettes (Optiglass, Hainault, UK). This allowed both INS and Raman spectra to be recorded without removing the sample from the cuvette. Powder X-ray diffraction of the compounds showed that there was unreacted RbH present in Rb_2PtH_6. In Rb_2PtD_6, no impurities were visible.

† Rutherford Appleton Laboratory.
‡ Max Planck Institut für Chemische Physik fester Stoffe.
§ Institut für Anorganische Chemie der TH Aachen.
|| University of Surrey.
⊥ Renishaw plc.
○ S.M.Bennington@rl.ac.uk.
A.J.Ramirez-Cuesta@rl.ac.uk.
▽ Aufferma@cpfs.mpg.de.
◆ Welf.Bronger@ac.rwth-aachen.de.
+ actinictech@dial.pipex.com.
∞ Ken.Williams@renishaw.com.
¶ Tim.Smith@renishaw.com.

(1) *Hydrogen in Intermetallic Compounds II*; Schlapbach, L., Ed.; Topics in Applied Physics, Vol. 67; Springer: 1992.
(2) Yvon, K.; In *Encyclopedia of Inorganic Chemistry*; King, R. B., Ed.; Wiley: New York, 1994; p 1401.
(3) Bronger, W.; Auffermann, G. *Chem. Mater.* **1998**, *10*, 273.
(4) Bronger, W.; Auffermann, G. *Z. Anorg. Allg. Chem.* **1995**, *621*, 1318.

10.1021/ja034323h CCC: $25.00

B. Raman Spectroscopy. FT−Raman spectra of the compounds were recorded with a Perkin-Elmer System 2000 spectrometer using an Nd:YAG laser at 1064 nm as the excitation source and a room temperature InGaAs detector. Spectra were recorded at 4 cm^{-1} resolution with 32 scans and with laser power in the range 50−150 mW. Spectra of Rb_2PtH/D_6 were also recorded with a Renishaw 2000 dispersive Raman microscope spectrometer with 633 nm excitation from a HeNe laser with 6 mW power at the sample and with 514.5 nm excitation from an Ar^+ laser with 3 mW power at the sample. The instrument has been described in detail elsewhere.[5]

C. INS Spectroscopy. The inelastic neutron scattering experiments were performed with the high resolution time-of-flight spectrometers, TOSCA (using both the first[6] and second[7] stages of its installation) and MARI,[8] at the ISIS pulsed spallation neutron source at the Rutherford Appleton Laboratory, Chilton, UK. While both TOSCA and MARI access the same energy transfer range, 0 to 4000 cm^{-1}, they provide complementary data. This arises from their different operating principles. In a time-of-flight spectrometer, to determine the energy transfer, the arrival time at the detector is required plus the flight time for either the incident or scattered neutron. This is equivalent to fixing either the final energy as done in TOSCA or fixing the incident energy as done in MARI. In TOSCA, the resolution is ∼1.5% of the energy transfer across the entire energy range, while, on MARI, it is ∼1% of the incident energy at the largest energy transfer and degrades with decreasing energy transfer. Thus, TOSCA provides excellent energy resolution at energy transfers < 1200 cm^{-1}, at larger energy transfer MARI provides better resolution.

There is another difference between the spectrometers. The observed intensity of an INS spectral band, S, is a function of both the energy, ω, and the momentum, Q, exchanged during the scattering process.

$$|\mathbf{k}| = 2\pi/\lambda$$

$$\mathbf{Q} = \boldsymbol{k}_{\text{scattered}} - \boldsymbol{k}_{\text{incident}} = \boldsymbol{k}_{\text{scat}} - \boldsymbol{k}_{\text{inc}}$$

$$Q = |\mathbf{Q}|$$

$$Q^2 = k^2_{\text{inc}} + k^2_{\text{scat}} - 2\,k_{\text{inc}}k_{\text{scat}}\cos(\theta) \qquad (1)$$

For TOSCA, k_{scat} is small so $Q^2 \approx k^2_{\text{inc}} \approx \omega/16.8$ (ω in cm^{-1} and Q in $Å^{-1}$), and the spectrometer follows a specific trajectory through (Q, ω) space. On MARI, this is not the case and the spectrometer has detectors covering the range of scattering angles 3−135° to allow simultaneous determination of both Q and ω. Thus, INS on MARI is intrinsically a two-dimensional spectroscopy.

The intensity, S, of an INS band is given by[9]

$$S(Q,n\omega_i) \propto \frac{(QU_i)^{2n}}{n!}\exp(-(QU_{\text{Tot}})^2)\sigma \qquad (2)$$

where ω_i is the ith mode at frequency ω; $n = 1$ for a fundamental, 2 for a first overtone or binary combination, 3 for a second overtone or ternary combination, and so forth; Q is the momentum transfer defined above; U_i is the root-mean-square displacement of the atoms in the mode; U_{Tot} is the total root-mean-square displacement of all the atoms in all the modes, both internal and external; and σ is the inelastic scattering cross-section of the atom. The total scattering cross-sections of hydrogen, deuterium, rubidium, and platinum are 82.0, 7.64, 6.6, and 11.78 barns (1 barn = 1×10^{-28} m^2), respectively,[10] and since the intensity is dependent on the amplitude of vibration, which is larger for light atoms, the spectra will be dominated by motions that involve displacement of hydrogen or deuterium, so much so that all other atoms may be neglected. The exponential term in eq 2 is a Debye−Waller factor, so to minimize this the spectra were run at low temperature (20K on TOSCA, 5K on MARI).

In inelastic neutron scattering, the intensity does not depend on electronic properties such as dipole moment or polarizability, so there are no symmetry-based selection rules and all modes are allowed. From a conventional Wilson−Decius−Cross[11] normal coordinate analysis, it is possible to calculate *both* the energies (from the eigenvalues) and intensities (from the eigenvectors) for INS spectra of molecular species. The program CLIMAX[12] has been developed to carry out the normal coordinate analysis using both energy and intensity information as constraints. Recently, a successor to CLIMAX, aCLIMAX,[13] has been implemented that uses the results from ab initio calculations to generate an INS spectrum that includes events that nominally contain up to four quanta.

In INS spectroscopy, overtones and combination bands are allowed transitions in the harmonic approximation, and combination bands (phonon wings) between internal modes and external (lattice) modes maybe particularly strong. Infrared and Raman bands are observed at zero wavevector (Brillouin zone center), whereas INS spectroscopy is sensitive to modes at all wavevectors across the Brillouin zone and acoustic modes may be observed.

The TOSCA INS spectra are available from the INS database[14] at www.isis.rl.ac.uk/insdatabase.

C. Computational Studies. Density functional theory (DFT) was used to study the isolated ion using the B3LYP functional with the SDD and LANL2DZ basis sets as implemented in GAUSSIAN98.[15] The complete unit cell was also investigated with the periodic DFT code DMOL3[16] as implemented in the Materials Studio package from Accelerys. The local density approximation (Perdew−Wang) was used with a localized basis set (DND double numerical), represented as a numerical tabulation. The vibrational spectra were calculated in the harmonic approximation using the finite displacement technique to obtain the dynamical matrix. Starting from an energy minimized geometry, each of the atoms in the unit cell was displaced by 0.005 Å in turn along the three Cartesian directions and a single-point calculation gives the Hellmann−Feynmann forces on all the atoms, from which the force constants are obtained by dividing by the displacement. Positive and negative displacements were used in order to obtain more accurate central finite differences. The force constant matrix F was transformed to mass-dependent coordinates by the G matrix giving the dynamical matrix. Diagonalization of the dynamical matrix gives the vibrational eigenvalues and eigenvectors.

DMOL3 performs geometry optimizations but not lattice optimizations. For each of the alkali metal salts, the geometry was energy minimized and the vibrational frequencies were calculated. The free energy is the sum of the electronic energy plus the zero-point energy,[17]

(5) Williams, K. P. J.; Pitt, G. D.; Smith, B. J. E.; Whitley, A.; Batchelder, D. N.; Hayward, I. P. *J. Raman Spectrosc.* **1994**, *25*, 131.
(6) Bowden, Z. A.; Celli, M.; Cilloco, F.; Colognesi, D.; Newport, R. J.; Parker, S. F.; Ricci, F. P.; Rossi-Albertini, V.; Sacchetti, F.; Tomkinson, J.; Zoppi, M. *Physica B* **2000**, *276−278*, 98.
(7) Colognesi, D.; Celli, M.; Cilloco, F.; Newport, R. J.; Parker, S. F.; Rossi-Albertini, V.; Sacchetti, F.; Tomkinson, J.; Zoppi, M. *Appl. Phys.* **2002**, *A 74* [*Suppl*], S64.
(8) Arai, M.; Taylor, A. D.; Bennington, S. M.; Bowden, Z. A. In *Recent developments in the physics of fluids*; Howells, W. S., Soper, A. K., Eds.; Adam Hilger: Bristol, 1992; F321−F328.
(9) Tomkinson, J. In *Neutron Scattering From Hydrogen In Materials*; Furrer, A., Ed.; World Press: Singapore, 1994; p 168.
(10) Sears, V. F. *Neutron News* **1992**, *3*, 26.
(11) Wilson, E. B., Jr.; Decius, J. C.; Cross, P. C. *Molecular Vibrations*; Dover: New York, 1955.
(12) Kearley, G. J. *Nucl. Instrum. Methods Phys. Res., Sect. A* **1995**, *354*, 5.
(13) Champion, D. J.; Tomkinson, J.; Kearley, G. J. *Appl. Phys. A*, [*Suppl.*] **2002**, S1302.
(14) Parker, S. F.; Champion, D. J. *Internet J. Vib. Spec.* **1999**, *3* [http://www.ijvs.com/volume3/edition3/section1.htm#Ed].
(15) Frisch, M. J.; Trucks, G. W.; Schlegel, H. B.; Scuseria, G. E.; Robb, M. A.; Cheeseman, J. R.; Zakrzewski, V. G.; Montgomery, J. A. Jr.; Stratmann, R. E.; Burant, J. C.; Dapprich, S.; Millam, J. M.; Daniels, A. D.; Kudin, K. N.; Strain, M. C.; Farkas, O.; Tomasi, J.; Barone, V.; Cossi, M.; Cammi, R.; Mennucci, B.; Pomelli, C.; Adamo, C.; Clifford, S.; Ochterski, J.; Petersson, G. A.; Ayala, P. Y.; Cui, Q.; Morokuma, K.; Malick, D. K.; Rabuck, A. D.; Raghavachari, K.; Foresman, J. B.; Cioslowski, J.; Ortiz, J. V.; Stefanov, B. B.; Liu, G.; Liashenko, A.; Piskorz, P.; Komaromi, I.; Gomperts, R.; Martin, R. L.; Fox, D. J.; Keith, T.; Al-Laham, M. A.; Peng, C. Y.; Nanayakkara, A.; Gonzalez, C.; Challacombe, M.; Gill, P. M. W.; Johnson, B.; Chen, W.; Wong, M. W.; Andres, J. L.; Gonzalez, C.; Head-Gordon, M.; Replogle, E. S.; Pople, J. A. *Gaussian 98*, revision A.3; Gaussian, Inc.: Pittsburgh, PA, 1998.
(16) Delley, B. *J. Chem. Phys.* **2000**, *113*, 7756.

Table 1. Classification[a] of Vibrations of Rb_2PtH_6

space group	$Fm3m$
formula units in Bravais cell	1
site symmetry	O_h
Pt−H stretches	A_{1g} (R) + E_g (R) + T_{1u} (IR)
Pt−H bends	T_{2g} (R) + T_{1u} (IR) + T_{2u} (ia)
libration	T_{1g} (ia)
translations	T_{2g} (R) + T_{1u} (IR)
acoustic	T_{1u} (ia)

[a] Activity shown in brackets: R = Raman active, IR = infrared active, ia = inactive in both Raman and infrared. Note *all* vibrations are allowed in the INS spectrum.

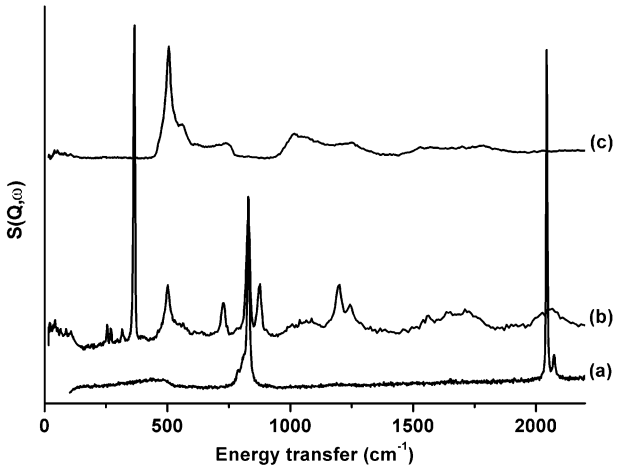

Figure 1. (a) Dispersive Raman and (b) TOSCA INS spectra of Rb_2PtH_6. (c) TOSCA INS spectra of RbH.

both of which are calculated by DMOL3. This was carried out for the experimental lattice parameter and with it at ±0.1 Å. A parabola was then fitted to the points, and the lattice parameter of the minimum energy position was determined; the structure and vibrational spectrum were then recalculated with this lattice parameter.

III. Results and Discussion

At room temperature, Rb_2PtH_6/D_6 crystallizes in the cubic space group $Fm\bar{3}m \equiv O_h^5$ (number 225, $a = 8.5369(1)$Å) with four formula units in the unit cell.[4] There is one formula unit in the Bravais cell, and the ions all lie on special sites (Pt in 4*a*, Rb in 8*c*, D in 24*e* with $x = 0.1908(2)$). Thus the Rb^+ ions are on tetrahedral T_d sites, and the PtH_6^{2-} ions are on octahedral O_h sites. Using the correlation method,[18] the vibrations can be classified as shown in Table 1.

The Raman and TOSCA INS spectra of Rb_2PtH_6 and Rb_2PtD_6 are shown in Figures 1 and 2, respectively. Also shown in Figure 1 is the INS spectrum of RbH, and it is clear that the feature at 493 cm^{-1} is due to the unreacted RbH detected by powder X-ray diffraction. We note that the spectrum of RbH is in reasonable agreement with that predicted from a lattice dynamics calculation of RbD.[19]

The INS spectra in Figures 1 and 2 are much richer because of the absence of selection rules. However, the selection rules allow straightforward symmetry assignments. It follows that the three Raman bands observed at 2074 (1487), 2044 (1466), and 829 (588) cm^{-1} (the values in brackets are for the deuterated

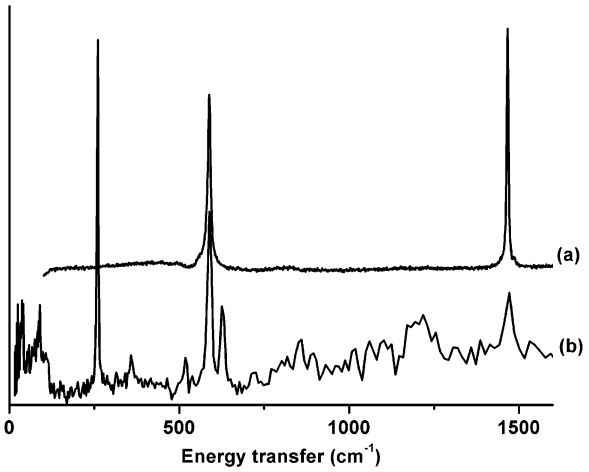

Figure 2. (a) Dispersive Raman and (b) TOSCA INS spectra of Rb_2PtD_6, 0−1600 cm^{-1}.

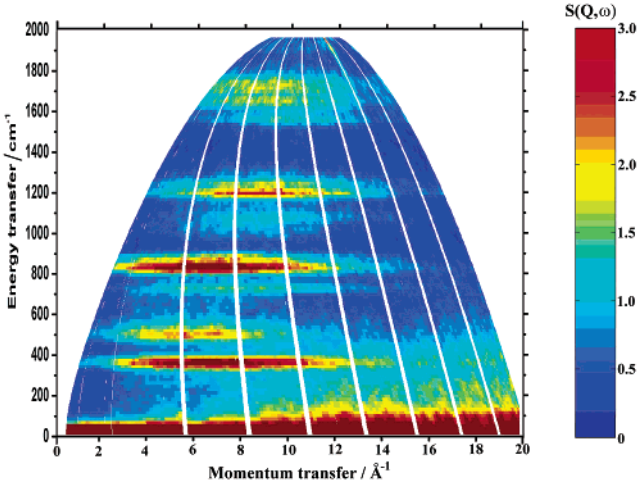

Figure 3. INS spectrum of Rb_2PtH_6 recorded using an incident energy of 2000 cm^{-1} on MARI.

complex) are the E_g, A_{1g}, and T_{2g} modes, respectively. There is a possible ambiguity in the assignment of the E_g and A_{1g} modes, but the intensities of the two modes strongly support the present assignment.

The INS spectrum of Rb_2PtH_6 recorded on the chopper spectrometer MARI with an incident energy of 2000 cm^{-1} is shown in Figure 3. Cuts at constant energy transfer are shown in Figure 4. It is apparent that the maximum in Q occurs at different values for different modes.

From differentiation of eq 2, the maximum in $S(Q,n\omega)$ occurs when

$$n = Q^2 U_{\mathrm{Tot}}{}^2 \qquad (3)$$

thus providing a method to distinguish fundamentals ($n = 1$) from higher order ($n \geq 2$) transitions such as overtones and combinations.

From the MARI data of Rb_2PtH_6, shown in Figures 3 and 4, the features at 368 and 829/877 cm^{-1} (the two modes at 829 and 877 cm^{-1} are not resolved in these data) have their maximum intensity at $Q \approx 6.5$ $Å^{-1}$; since these occur at the lowest Q, it follows from eq 3 that they must be fundamentals. The feature centered at 1200 cm^{-1} has its maximum at $Q \approx 9.0$ $Å^{-1} \approx (6.5 \times \sqrt{2})$ $Å^{-1}$ and thus must be an $n = 2$ process

(17) Taylor, M. B.; Barrera, G. D.; Allan, N. L.; Barron, T. H. K.; Mackrodt, W. C. *Comp. Phys. Commun.* **1998**, *109*, 135.
(18) Fateley, W. G.; Dollish, F. R.; McDevitt, N. T.; Bentley, F. F. *Infrared and Raman Selection Rules for Molecular and Lattice Vibrations*: *The Correlation Method*; Wiley-Interscience: New York, 1972.
(19) Dyck, W.; Jex, H. *J. Phys. C*: *Solid State Phys.* **1981**, *14*, 4193.

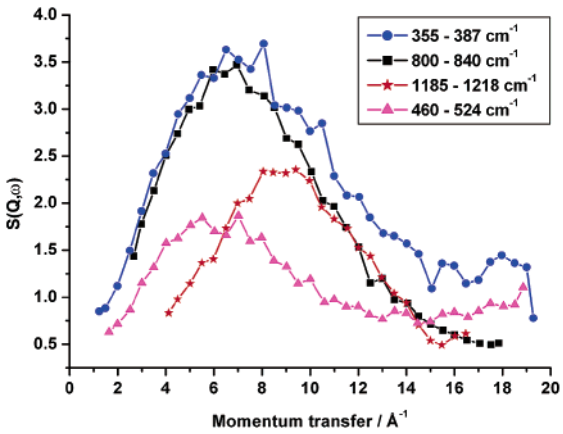

Figure 4. Cuts at constant energy transfer of the MARI INS spectrum of Rb_2PtH_6.

(first overtone or binary combination). The feature near 500 cm^{-1} has its maximum intensity at $Q \approx 5.8$ $Å^{-1}$ implying $n < 1$, a logical contradiction. This is the strongest band of the RbH impurity so will have a different value of U_{Tot}^2 and hence a different maximum in Q. Thus the technique also allows the presence of impurities to be recognized.

In a very elegant study, Preetz et al.[20] were able to obtain the infrared and Raman spectra of K_2PtH_6 and its isotopomers and also of A_2PtD_6 (A = Na, K, Rb). For K_2PtH_6, this showed that the T_{2g} and T_{1u} bending modes are at 840 and 881 cm^{-1}, respectively. Since in the present case the T_{2g} mode is at 829 cm^{-1}, we assign the T_{1u} mode to the band at 877 cm^{-1}. This leaves one bending mode unaccounted for. A diagonal force field indicates that the three bending modes should occur at similar energies and have very similar intensities. In the present case, the 829 cm^{-1} band is almost exactly twice as intense as the 877 cm^{-1} band (see Figures 1b and 6a); thus, the third internal mode of T_{2u} symmetry must be accidentally degenerate with the T_{2g} mode at 829 cm^{-1}.

The remaining internal mode is the T_{1u} stretching mode. In the infrared spectrum[20] of K_2PtH_6, three bands are observed at 1748, 1702, and 1648 cm^{-1}. The presence of three bands could be the result of a reduction in symmetry that removes the degeneracy of the T_{1u} mode. This is not supported by either the crystallography[21] or the fact that none of the other T modes are split. Since the band at 1748 cm^{-1} is the strongest, we assign this to the T_{1u} fundamental and the other two bands to overtones or combinations whose intensity is enhanced by Fermi resonance.

For the rubidium salt, the situation is similar. In Figure 1b, a complex envelope with at least three maxima is visible in the range 1400−1900 cm^{-1}. In this region, MARI offers better resolution. Figure 5 shows this range and that more modes are apparent; the figure also shows its resolution as a sum of Gaussian lines. From Figure 3, since the modes occur at higher Q than the fundamentals, this confirms that most of the intensity is due to overtones or combinations, although the T_{1u} fundamental must be present. The infrared spectrum[20] of Rb_2PtD_6 has the strongest band at 1235 cm^{-1}, which is assigned to the T_{1u} fundamental; the isotope shift for the same mode in K_2PtH_6 K_2PtD_6 is 1.40, and assuming the same ratio, the corresponding mode in Rb_2PtH_6 is predicted at 1726 cm^{-1}. Accordingly, the band at 1728 cm^{-1}, band 6 in Figure 5, is assigned to the T_{1u} fundamental.

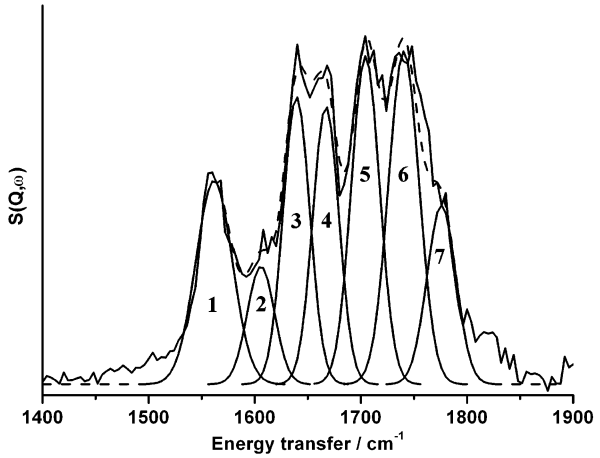

Figure 5. Region 1400−1900 cm^{-1} of the INS spectrum of Rb_2PtH_6 using only the low angle detectors on MARI, i.e., at low momentum transfer. The fit (dashed line) to a sum of Gaussian peaks is also shown (the assignments are given in Table 2). The T_{1u} stretching mode is peak 6.

Table 2. Observed Bands (cm^{-1}) and Assignments for Rb_2PtH_6 and Rb_2PtD_6 in O_h Symmetry

Raman		INS		
H	D	H	D	assignment[a]
2074w	1487w			ν_2Pt−H/D stretch (E_g)
2044vs	1466vs			ν_1Pt−H/D stretch (A_{1g})
		1775w		2 ν_4 {7}
		1743m		ν_3Pt−H/D stretch (T_{1u}) {6}
1700vw		1708m		($\nu_5 + \nu_4$) and ($\nu_6 + \nu_4$) {5}
		1669m		2 ν_5 and 2 ν_6 {4}
1648vw		1640m		2 ν_5 and 2 ν_6 {3}
		1603w		(2 × Lib + ν_4) {2}
1573vw		1563m		(2 × Lib + ν_5) and (2 x Lib + ν_6) {1}
		1240m		(Lib + ν_4)
		1193s	860m	(Lib + ν_5) and (Lib + ν_6)
		877s	631s	ν_4 Pt−H/D bend (T_{1u})
829s	588s	828vs	592vs	ν_5 *Pt−H/D bend* (T_{2g}) and ν_6 Pt−H/D bend (T_{2u})
		726m	521w	2 × Lib
		366vs	262vs	libration (T_{1g})
		90w	90w	translation (T_{2g})
		108/65w	76w	optic translation (T_{1u})
		40w	38w	acoustic translation (T_{1u})

[a] Where more than one assignment is given, the italicisized one is that of the Raman band. Numbers in braces refer to the peaks shown in Figure 5. s = strong, m = medium, w = weak, br = broad, v = very.

The four remaining fundamental modes are the external modes, the T_{1g} libration and the translations: a T_{1u} acoustic mode and optic T_{1u} and T_{2g} modes. Since the libration only involves hydrogen motion, it will occur at higher energy than the translations; also, it is usually of similar intensity to the bending modes and will also show the full $1/\sqrt{2}$ isotope shift. Accordingly, the very sharp 368 cm^{-1} feature with a deuterium counterpart at 259 cm^{-1} is so assigned. For the translational modes, only three modes are expected but there are four clear maxima in the spectrum of the protonated compound, Table 2. In the deuterated compound, the peaks at 108 and 65 cm^{-1} have diminished in relative intensity. The T_{2g} mode only involves motion of the Rb^+ ions, and the peak at 90 cm^{-1} is assigned to this mode. The acoustic mode is generally the lowest energy mode and so is assigned to the 42 cm^{-1} feature. The optic T_{1u} mode is assigned to the bands at 108 and 65 cm^{-1}. To account for the presence of two bands, it is necessary to assume that this mode is dispersed.

(20) Bublitz, D.; Peters, G.; Preetz, W.; Auffermann, G.; Bronger, W. *Z. Anorg. Allg. Chem.* **1997**, *623*, 184.
(21) Bronger, W.; Auffermann, G. *Angew. Chem., Int. Ed. Engl.* **1994**, *33*, 1112.

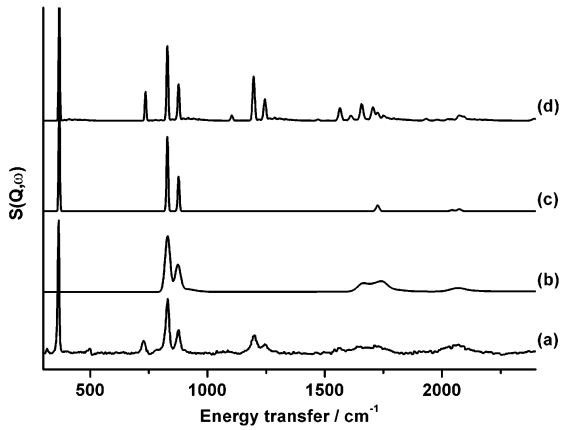

Figure 6. Comparison of (a) observed spectrum of Rb_2PtH_6 (the spectrum of RbH has been subtracted from the TOSCA spectrum, the derivative-like feature at 500 cm^{-1} is due to a slight miscancellation) with (b) CLIMAX fit, (c) aCLIMAX fit including the T_{1g} librational mode, and part d as part c but with inclusion of overtones and combinations of up to four quanta.

For the internal modes, we have used CLIMAX[12] to fit a force field to the observed INS spectrum, Figure 6a (after subtraction of the RbH spectrum), as shown in Figure 6b. This shows that several of the modes are unaccounted for and are most likely combinations with the librational mode. To include this, one method is to expand the model to include the presence of other ions, as was done for a series of A_xPdH_y salts[22] and Mg_2NiH_4 and Rb_3ZnH_5.[23] As an alternative, the force field was used to generate a set of atomic displacements for the internal modes, the displacements for the T_{1g} librational mode were included, and the whole was used as input to the program aCLIMAX.[13] The result is shown in Figure 6c for the fundamentals and in Figure 6d after inclusion of overtones and combinations of up to four quanta. This allows an immediate assignment of all the remaining features in the spectrum except for the weak bands at 246, 259, and 311 cm^{-1}. These have no obvious deuterium counterparts and may represent a small quantity of an impurity. An alternative possibility is that they are three quanta overtones and/or combinations of lattice modes in Fermi resonance with the extremely strong librational mode at 364 cm^{-1}. They are not observed in the deuterated spectrum partly because of the poorer signal-to-noise level resulting from the smaller cross-section of deuterium and partly because of overlap with the 259 cm^{-1} librational mode of the deuterated ion. Table 2 lists the frequencies and assignments of all the observed bands, and it is clear that the system is almost harmonic.

For the bands in the region of the T_{1u} stretching mode, a check on the assignments is possible. From consideration of the possible overtones and combinations, there are six that can occur in this region. Three of these ($2 \times$ Lib + ν_6), ($2 \times$ Lib + ν_4), and ($\nu_5 + \nu_4$), have components of T_{1u} symmetry that can theoretically gain intensity via Fermi resonance with the T_{1u} fundamental. The ($2 \times$ Lib + ν_6) combination involves an infrared inactive mode and a forbidden mode and so would not be expected to have any intensity. The other two modes involve the allowed infrared active T_{1u} ν_4 fundamental and so are observed. Assuming that the same situation applies to the potassium salt, this allows an approximate value for the librational mode of 379 cm^{-1} to be deduced for the potassium salt. For the A_{1g} and E_g stretching modes, no extra bands are observed in the Raman spectrum, although additional bands are present in the INS spectra. Consideration of the combinations that occur in this region shows that none of them involve Raman active fundamentals that have A_{1g} components and so would not be expected to have any intensity.

Table 3. Comparison of Observed and Calculated Frequencies (cm^{-1}) for Rb_2PtH_6

	GAUSSIAN98			
mode	LANL2DZ	SDD	DMOL3[a]	observed
ν_2Pt−H stretch (E_g)	1959	1949	2246, 2246, 2245, 2245	2074
ν_1Pt−H stretch (A_{1g})	1959	1956	2244, 2244, 2244, 2244	2044
ν_3Pt−H stretch (T_{1u})	1560	1516	1978, 1963, 1963, 1957	1743
ν_4 Pt−H bend (T_{1u})	710	730	841, 840, 837, 825	877
ν_6 Pt−H bend (T_{2u})	670	680	804, 804, 798, 794	828
ν_5 Pt−H bend (T_{2g})	756	748	789, 788, 787, 785	828
libration (T_{1g})			304, 299, 292, 287	366
optic translation (T_{1u})			97, 87, 87, 85	108/65
optic translation (T_{2g})			80, 76, 58, 56	90
acoustic translation (T_{1u})			56,54,54,0	42

[a] Four frequencies are given because DMOL3 carries out the calculation in *P*1 symmetry.

The librational and bending modes of the complex in the TOSCA INS spectrum are extremely narrow with a full width at half-maximum of 5.8, 11.5, and 13.3 cm^{-1} for the 365, 826, and 872 cm^{-1} mode, respectively. The widths are all resolution limited and are the narrowest bandwidths measured by INS in this spectral region to date. They are also a demonstration of the resolution that is obtainable with state-of-the art instrumentation. Since the INS spectrum is a measurement of the density-of-states which is the projection of the dispersion curves onto the energy axis, the narrowness demonstrates that the modes are essentially dispersionless.

To provide confirmation of the assignments we have carried-out DFT calculations of the isolated $[PtH_6]^{2-}$ ion. Unsurprisingly, the results are poor. The Pt−H bond length is overestimated at 1.678 Å (experimental is 1.629 Å) and the frequencies are underestimated, see Table 3. The pattern is correctly reproduced (bending modes in a narrow range, T_{1u} stretching mode separated from the A_{1g} and E_g stretching modes), but the symmetry assignments are incorrectly ordered.

Much better results are obtained with the periodic DFT code DMOL3. The Pt−H bond distance is better, 1.646 Å, and as Table 3 and Figure 7a show, the frequency agreement is much better. There are more modes than expected because DMOL3 carries out the computations in *P*1 symmetry; thus, there are four formula units in the unit cell. However, the frequencies are predicted in the correct order; in particular, the T_{2u} and T_{2g} modes are almost degenerate as found experimentally. Shifting the calculated frequencies to the experimental ones, a process analogous to scaling as described elsewhere,[24] together with inclusion of up to four quanta events, generates the spectrum shown in Figure 7b. It can be seen that the result is in excellent agreement with the experimental spectrum, Figure 7c, and provides complete confirmation of the assignments.

Having established that periodic DFT gives a reasonable description of the structure, we have carried out a series of calculations on all the A_2PtH_6 (A = alkali metal) compounds to investigate the bonding present. In addition to the Rb salt, the compounds with A = Na,[25] K,[21] and Cs[4] are known and

(22) Olofsson-Mårtensson, M.; Häussermann, U.; Tomkinson, J.; Noréus, D. *J. Am. Chem. Soc.* **2000**, *122*, 6960.
(23) Parker, S. F.; Williams, K. P. J.; Smith, T.; Bortz, M.; Bertheville, B.; Yvon, K. *Phys. Chem. Chem. Phys.* **2002**, *10*, 1732.
(24) Ramirez-Cuesta, A. J.; Tomkinson, J. *Neutron News*, accepted for publication.

Table 4. Comparison of Properties of A_2PtH_6 (A = Li, Na, K, Rb, Cs)[a]

property	Li	Na	K	Rb	Cs	gas phase[b]
lattice parameter (Å)	6.564 (6.5549)[c]	7.1716 (7.3410)	8.2002 (8.1399)	8.6222 (8.5369)	8.9503 (8.9681)	
Pauling ionic radius A (Å)	(0.60)	(0.95)	(1.33)	(1.48)	(1.69)	
lattice energy (kJ mol^{-1})	2223	1966	1755	1665	1577	
Pt−H (Å)	1.639	1.641 (1.615)	1.644 (1.640)	1.646 (1.629)	1.647 (1.641)	1.678
A−H (Å)	2.354	2.540 (2.74)	2.927 (3.12)	3.091 (3.06)	3.219 (3.52)	
ν_1Pt-D stretch A_{1g} (cm^{-1})	1673	1651 (1491)	1604 (1471)	1588 (1466)	1577	1387
charge on Pt	−1.718	−1.777	−1.601	−1.511	−1.422	−1.860
charge on A	+0.370	+0.598	+0.698	+0.703	+0.536	
charge on H	+0.163	+0.097	+0.034	+0.018	+0.058	−0.232

[a] Experimental values in parentheses. [b] Average of SDD and LANL2DZ results. [c] By extrapolation of the Na, K, Rb, and Cs salts.

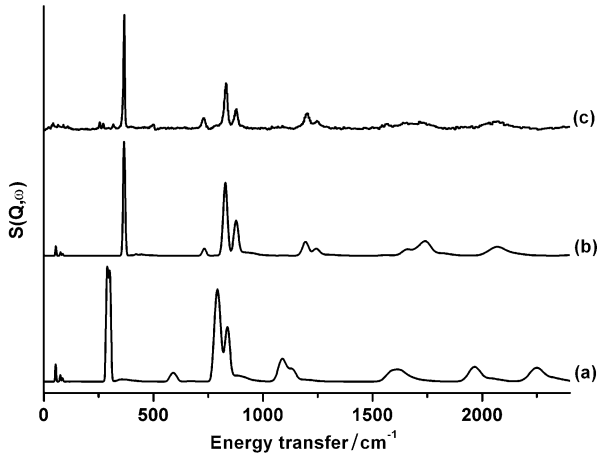

Figure 7. (a) Displacements from DMOL3 used in aCLIMAX to generate the INS spectrum. First overtones and binary combinations are included. (b) "Scaled" DMOL3 (overtones and combinations up to four quanta are included) and (c) experimental INS spectra of Rb_2PtH_6.

have been structurally characterized. The Li salt is, at present, unknown: attempts to synthesize it using similar conditions (1250 bar, 820 K) to those employed for the other alkali metals resulted in the very unusual compound $Li_5Pt_2H_9$,[26] which contains square-prismatic $[H_4Pt-H-PtH_4]^{5-}$ ions. A plot of Pauling ionic radius versus lattice parameter of the Na, K, Rb, and Cs salts gave a straight line with a correlation coefficient of 0.9985; this was used to estimate a lattice parameter of 6.5549 Å for the Li salt.

As described, in the Experimental Section, the geometry was optimized at the free energy minimum. Using this structure, the vibrational frequencies and the charge on the ions were calculated. The results are shown in Table 4. Stable structures were obtained for all the counterions including Li. The lattice energy of the salts was calculated using the method of Jenkins et al.;[27] the results, Table 4, support the idea that the Li salt should be stable. It is likely that $Li_5Pt_2H_9$ is an intermediate on the path to Li_2PtH_6; more forcing conditions, particularly higher pressure, would be an avenue to pursue.

From Table 4, it can be seen that the DMOL3 results mirror the experimental trends. The Pt−H and A−H bond distances increase with increasing cation size. As may be expected, as the Pt−H distance increases, the Pt−H stretching frequency falls The Pt−H bonding is largely covalent in the salts since the distances are close to the sum of the covalent radii (1.65 Å) and are similar to those found for platinum hydride complexes, ~1.61 Å.[28] This is confirmed by inspection of the Mulliken charges which shows that the Pt carries a sizable negative charge and the hydrogen, only a small positive charge in the salts. Note the distinction from the gas phase where the hydrogen carries a negative charge. Thus, the Pt−H bonding is largely covalent, but there is an ionic component. The role of the alkali metal ion is to reduce the charge on the Pt and H, thus stabilizing the complex. As the alkali metal becomes more electropositive, it has an increasing charge. Surprisingly, this trend is apparently not continued with Cs.

The role of the cation to stabilize the complex by reducing the charge on the metal and hydrogen has been observed before in the complex Mg_2NiH_4[29] which contains Ni(0) and in a series of Pd(0) hydrides.[22] While this is the first time it has been shown in a formally high valent complex, it suggests that this is the general case. This would also explain the empirical observation that it is generally easier to make the complexes with K and Cs than with Li or Na.

IV. Conclusions

The present work has provided a complete set of assignments for the vibrational spectrum of Rb_2PtH_6 and Rb_2PtD_6. The use of DMOL3 to analyze the spectra provides confirmation of the assignments and sets a standard for future work in this area. We believe, that this is the first time a periodic DFT code has been applied to the analysis of the INS spectrum of an ionic material. The work has also provided an explanation for the unusual infrared spectrum of the potassium salt. The DFT studies have also highlighted the crucial role of the cation in removing charge from the transition metal and "hydride" ligand. It is suggested that this is a general occurrence.

The most significant aspect of the work is the use of the momentum transfer information provided by an INS chopper spectrometer. The straightforward method employed for the analysis of the data is applicable to *any* molecular system (organic or inorganic) and demonstrates the potential of these instruments for chemistry. The availability of INS instrumentation will dramatically increase over the next five years or so with the construction of a second target station at ISIS (Chilton, UK),[30] the Spallation Neutron Source, SNS (Oak Ridge, USA),[31] and J-PARC (Tokai, Japan).[32] Each installation will have at least one chopper instrument and one TOSCA-like instrument.

Acknowledgment. The Rutherford Appleton Laboratory is thanked for access to neutron beam facilities.

JA034323H

(25) Bronger, W.; Auffermann, G. *J. Alloys Compd.* **1995**, *219*, 45.
(26) Bronger, W.; à Brassard, L. *Angew. Chem., Int. Ed. Engl.* **1995**, *34*, 898.
(27) Jenkins, H. D. B.; Roobottom, H. K.; Passmore, J.; Glasser, L. *Inorg. Chem.* **1999**, *38*, 3609.
(28) Bau, R.; Drabnis, M. H. *Inorg. Chim. Acta*, **1997**, *259*, 27.
(29) Häussermann, U.; Blomqvist, H.; Noréus, D. *Inorg. Chem.* **2002**, *41*, 3684.
(30) http://www.isis.ac.uk/ targetstation2/.
(31) http://www.sns.gov.
(32) http://jkj.tokai.jaeri.go.jp/.